IV International Conference on Particle-based Methods – Fundamentals and Applications
PARTICLES2015
E. Oñate, M. Bischoff, D.R.J. Owen, P. Wriggers & T. Zohdi (Eds)

THEORETICAL INVESTIGATION OF THE DYNAMICS OF FRICTION STIR WELDING PROCESS BY MOVABLE CELLULAR AUTOMATON METHOD

SERGEY V. ASTAFUROV[1,2], EVGENY V. SHILKO[1,2], EVGENY A. KOLUBAEV[1,3], ANDREY I. DMITRIEV[1,2], ANTON YU. NIKONOV[1,2], SERGEY G. PSAKHIE[1,3]

[1] Institute of Strength Physics and Materials Science SB RAS (ISPMS SB RAS)
2/4, Akademicheskii ave., 634055 Tomsk, Russia
e-mail: svastafurov@gmail.com , web page: http://www.ispms.ru

[2] National Research Tomsk State University (TSU)
36, Lenin ave., 634050, Tomsk, Russia
web page: http://www.tsu.ru

[3] National Research Tomsk Polytechnic University (TPU)
30, Lenin ave., 634050, Tomsk, Russia
web page: http://www.tpu.ru

Key words: Friction Stir Welding, Movable Cellular Automaton Method, Welded Joint, Porosity, Technological Process Parameters.

Summary. The paper is devoted to development of a new approach to study of friction stir welding (FSW) process on the mesoscopic scale. This approach is based on computer-aided simulation by movable cellular automaton (MCA) method. In the framework of developed formalism of MCA method the dynamics of the friction stir welding process of duralumin plates was investigated. It was shown that ratio of rotation velocity to velocity of translation motion of rotating tool greatly influences the quality of welded joint. Optimal choice of the ratio of these parameters could significantly decrease volume content of pores and microcracks in the welded joint.

1 INTRODUCTION

Friction stir welding (FSW) is a relatively new method of obtaining non-detachable joints of materials [1,2]. Recent year studies have shown that FSW is an effective way to obtain high quality joints for structures of various dimensions and shapes, including sheets, 3D profile structures, and pipes. Possessing the broad technological capabilities for obtaining permanent joints of details or units, it can be used as an alternative to riveted joints, electric arc welding, electron beam and laser welding as well as for welding the dissimilar materials. Thus, FSW becomes a perspective technology that has a great potential in various industries, including aerospace area.

The FSW technology is based on the friction of the rotating cylindrical or specially shaped tool between two connected or overlapped faces (ends) of metal plates [1-3]. The rotating tool is introduced into the joint of two metal plates to a depth approximately equal to their thickness. As a result of sliding friction (while rotating of the tool) a frictional heating the metal takes place. This leads to plastic deformation, flow and mixing of the material and, consequently, to formation of welded joint. The main problem when using FSW technology for producing of welded joints is the determination of an optimal regime (optimal parameters) of the rotating tool movement (in particular, the ratio of the angular and translational velocities of the tool). These parameters are determined by a wide range of factors, among which are the physical and mechanical properties of welded materials, the thickness of the connected plates, etc. Note, that incorrect determination of welding parameters is likely to cause of a large amount defects at different scales (pores, microcracks, etc.) in a weld seam and, consequently, to decrease of the quality of the joint [1-3].

Experimental determination of the parameters of FSW process is quite difficult task, because it requires obtaining and analysis of large amounts of data. In this regard, it is promising to use computer-aided simulation of process of formation of the welded joint. Since FSW processes are inseparably linked with the intensive formation of discontinuities, the generation of structural defects of different levels, the mass transfer, etc. the most preferable one is to use methods of discrete description of the simulated technology. In this paper, the dynamics of the FSW process of duralumin plates was investigated on the base of computer-aided simulation by the movable cellular automaton (MCA) method [4-7].

2 FORMALISM OF MOVABLE CELLULAR AUTOMATON METHOD

MCA method is the representative of the class discrete elements methods (DEM) and refers to subclass of simply deformable discrete elements [8,9]. In the framework of DEM simulated object on the considered scale is represented by ensemble of interacted elements of defined size and shape. In the process of loading a form of discrete elements may vary. The main feature of the method of simply deformable discrete elements is approximation of a uniform distribution of strains and stresses in the bulk of the discrete elements (in our case of the movable cellular automata). This approach imposes the requirement of proximity of initial linear discrete element size in different directions (in 2D case examples are the elements of round, square or hexagonal shape). In the framework of the described approach description of the evolution of the ensemble of interacting movable cellular automata is based on the numerical solution of the equations of Newton-Euler for centers of mass of the elements:

$$\begin{cases} m_i \dfrac{d^2\vec{R}_i}{dt^2} = \sum\limits_{j=1}^{N_i}\left(\vec{F}_n^{ij} + \vec{F}_\tau^{ij}\right) \\ \hat{J}_i \dfrac{d^2\vec{\theta}_i}{dt^2} = \sum\limits_{j=1}^{N_i}\vec{M}_{ij} \end{cases} . \qquad (1)$$

Here $\vec{R}_i$ and $\vec{\theta}_i$ are radius-vector and rotation angle of the automaton i, m_i and $\hat{J}_i$ are the mass and moment of inertia of the automaton, $\vec{F}_n^{ij}$ and $\vec{F}_\tau^{ij}$ are the forces of central and tangential interaction between automaton i and its neighbor j, $\vec{M}_{ij}$ is the momentum of force, N_i is the number of interacting neighbors.

The form of the equations for the interautomata interaction forces is borrowed from the embedded atom method [10,11] and contains a pair-wise and volume-dependent components:

$$m_i \frac{d^2\vec{R}_i}{dt^2} = \vec{F}_i = \left(\sum_{j=1}^{N_i} \vec{F}^{ij}_{pair} + \vec{F}^i_{\Omega} \right). \tag{2}$$

Here $\vec{F}_i$ is a total force, acting on automaton i from the surrounding elements, $\vec{F}^{ij}_{pair}$ and $\vec{F}^i_{\Omega}$ are its pair-wise (determined by the relative displacement of automata in pairs i-j) and volume-dependent (determined by the joint influence of the surroundings of the automaton i) components.

When modeling the FSW process at the mesoscopic scale (10 mm - 10 mm) it is adequate to consider of simulated metal as an isotropic medium. For locally isotropic materials volume-dependent component $\vec{F}^i_{\Omega}$ in relation (2) can be expressed in terms of the pressure P_i in the volume the automaton:

$$\vec{F}^{\Omega}_i = -A_i \sum_{j=1}^{N_i} P_j S_{ij} \vec{n}_{ij} \,. \tag{3}$$

Here S_{ij} is the area of interaction of elements i and j (area of plane face), A_i is the material parameter for the element i (in general case each distinct element simulates a material volume with unique phase or chemical composition and is characterized by a unique value of material parameter A), $\vec{n}_{ij}$ is a unit-vector. In this case, the expression for the central and the tangential forces of interaction of automaton i with the adjacent the automaton j in (1) have the following general form:

$$\begin{cases} F^{ij}_n = F^{ij}_{pair,n}\left(h_{ij}\right) - A_i P_i S_{ij} \\ F^{ij}_{\tau} = F^{ij}_{pair,\tau}\left(l_{ij}\right) \end{cases}, \tag{4}$$

where $F^{ij}_{pair,n}$ and $F^{ij}_{pair,\tau}$ are the central and tangential components of pair-wise potential interaction force $\vec{F}^{ij}_{pair}$. These components depend on the values of element i contributions to pair overlap h_{ij} and relative shear displacement l_{ij} respectively.

The specific form of dependencies $F^{ij}_{pair,n}\left(h_{ij}\right)$ and $F^{ij}_{pair,\tau}\left(l_{ij}\right)$ is directly connected with the type and parameters of the equation of state of the simulated material. Within the framework of the used approximation of locally isotropic material elastic interaction of movable cellular automata is described by linear Hooke's law for isotropic materials. The corresponding expressions for the forces of the central and the tangential linear-elastic interaction of movable cellular automata i and j are as follows [4-7]:

$$\begin{cases} \sigma^{cur}_{ij} = \sigma^{cur}_{ji} = \sigma^{pre}_{ij} + \Delta\sigma_{ij} = \sigma^{pre}_{ij} + 2G_i \Delta\varepsilon_{i(j)} + \left(1 - \dfrac{2G_i}{K_i}\right)\Delta\bar{\sigma}^i_{mean} \\ \Delta h_{ij} = \Delta\varepsilon_{i(j)} \, d_i/2 + \Delta\varepsilon_{j(i)} \, d_j/2 \end{cases}, \tag{5}$$

$$\begin{cases} \tau_{ij}^{cur} = \tau_{ij}^{pre} + \Delta\tau_{ij} = \tau_{ij}^{pre} + 2G_i\Delta\gamma_{i(j)} = \tau_{ji}^{cur} = \tau_{ji}^{pre} + \Delta\tau_{ji} = \tau_{ji}^{pre} + 2G_j\Delta\gamma_{j(i)} \\ \Delta l_{shear}^{ij} = \Delta\gamma_{i(j)} d_i/2 + \Delta\gamma_{j(i)} d_j/2 \end{cases}. \tag{6}$$

Here, relations for calculating the central and tangential interaction forces are written in increments (in hypoelastic form); the upper indexes ‘‘cur’’ and ‘‘pre’’ denote values of specific respond forces at the current and previous time steps of integrating the motion equation (1); Δ is the increment of corresponding parameter during one time step Δt, $\varepsilon_{i(j)}$ and $\varepsilon_{j(i)}$ are the central strains of automata i and j in pair i-j; $\gamma_{i(j)}$ and $\gamma_{j(i)}$ are the shear strains of automata i and j in the pair; G_i and K_i are the shear and bulk moduli of material filling the element i; $\overline{\sigma}_{mean}^{i} = -P_i$ is the average stress in the bulk of automaton i; $\sigma_{ij} = F_n^{ij}/S_{ij}$ and $\tau_{ij} = F_\tau^{ij}/S_{ij}$ are the relative values of central (F_n^{ij}) and tangential (F_τ^{ij}) interaction forces.

Average stresses $\overline{\sigma}_{mean}^{i}$ in (5) are calculated in terms of the diagonal components of the average stress tensor in the volume of automata $\overline{\sigma}_{\alpha\beta}^{i}$. Components $\overline{\sigma}_{\alpha\beta}^{i}$ are calculated using forces of interaction of automaton i with surroundings [4-7]:

$$\overline{\sigma}_{\alpha\beta}^{i} = \frac{1}{\Omega_i}\sum_{j=1}^{N_i} S_{ij} q_{ij} \left(\vec{n}_{ij}\right)_\alpha \left[\sigma_{ij}\left(\vec{n}_{ij}\right)_\beta + \tau_{ij}\left(\vec{t}_{ij}\right)_\beta\right], \tag{7}$$

where $\alpha,\beta = x,y,z$ (XYZ is the laboratory coordinate system), Ω_i is the automaton volume, $\left(\vec{n}_{ij}\right)_\alpha$ and $\left(\vec{t}_{ij}\right)_\alpha$ are the projection of the normal and tangential unit vectors in a pair on the axis of α of the laboratory coordinate system.

For the description of inelastic deformation of movable cellular automata theory of plastic flow with von Mises yield surface criterion is used [4-6]. Implementation of this theory carried out using the algorithm radial return algorithm of Wilkins [12]. In the framework of radial return algorithm the calculation of forces interautomaton interaction σ_{ij} и τ_{ij} at each time step of numerical integration of the equations of motion (1) is carried out in two stages. At the first step the current values of the interaction forces are calculated in the elastic approach (using equations (5) - (6)). At the end of this stage, the current value of the second invariant $\overline{\sigma}_{eq}^{i}$ of the average stress deviator $\overline{D}_{\alpha\beta}^{i} = \overline{\sigma}_{\alpha\beta}^{i} - 1/3\,\overline{\sigma}_{kk}^{i}\delta_{\alpha\beta}$ ($\overline{\sigma}_{\alpha\beta}^{i}$ are calculated in accordance with (7), using the current values of σ_{ij} and τ_{ij}) is compared with a threshold value σ_{pl}^{i}, which is corresponds to a point on the limit surface. In the case of fulfillment of inequality $\overline{\sigma}_{eq}^{i} > \sigma_{pl}^{i}$ the calculated at elastic stage values of specific forces σ_{ij} and τ_{ij} are corrected:

$$\begin{cases} \sigma_{ij}' = \left(\sigma_{ij} - \overline{\sigma}_{mean}^{i}\right)M_i + \overline{\sigma}_{mean}^{i} \\ \tau_{ij}' = \tau_{ij} M_i \end{cases}, \tag{8}$$

where $M_i = \sigma_{pl}^{i}/\overline{\sigma}_{eq}^{i}$. Note that relation (8) provides reduction of average stresses $\overline{\sigma}_{\alpha\beta}^{i}$ in the volume of movable cellular automaton to the desired point of the yield surface [4-6].

The rheological properties of the material of the movable cellular automaton i are determined by the defined curve $\bar{\sigma}^i_{eq} = \Phi(\bar{\varepsilon}^i_{eq})$, where $\bar{\varepsilon}^i_{eq}$ is the second invariant of the average strain deviator in the volume of the automaton [4-6]. This formulation corresponds to the approximation that plasticity is independent on the strain rate and is correct for the interval of loading parameters used in numerical modeling of FSW.

The major advantage of the formalism of DEM is the possibility of a discrete element to change its surrounding. This allows to explicitly consider the processes of fracture and restoration of the chemical bonds between the fragments of material that are be modeled by individual elements.

The fracture in the DEM is simulated by switching the state of the pair of interacting discrete elements from the chemically bound (linked) state to unlinked one. In unlinked pairs of discrete elements contact interaction is possible only, including force of resistance to compression and force of dry/viscous friction. Switching from a linked state to unlinked one is criterial. When modeling FSW process by MCA method the two-parameter fracture criterion of Drucker-Prager was used in the following form:

$$\sigma^{ij}_{eq} 0.5(a+1) + \sigma^{ij}_{mean} 1.5(a-1) = \sigma_c \, , \tag{9}$$

where σ^{ij}_{eq} and σ^{ij}_{mean} are invariants of stress tensor $\sigma^{ij}_{\alpha'\beta'}$ [4-6]; σ_c is compressive strength of pair *i-j*, $a = \sigma_c / \sigma_t$ is the ratio of compressive strength to tensile one.

Viscous character of fracture of plastic materials is taken into account by the introduction of the kinetics of bond breaking for pairs of automata, for which the condition $\sigma^{ij}_{eq} 0.5(a+1) + \sigma^{ij}_{mean} 1.5(a-1) > \sigma_c$ is satisfied. In this kinetic model is assumed that debonding in the pair of automata occurs gradually and is characterized by a decrease in linked portion of the interaction surface. The share of linked surface portion k^{ij}_{link} ($0 \le k^{ij}_{link} \le 1$) defines the current value of the surface area of interaction $S_{ij} = S^0_{ij} k^{ij}_{link}$ (S^0_{ij} is the surface area of the completely linked pair), which is used to calculate forces of interautomaton interaction and average stress tensor. Dynamics of changes of k^{ij}_{link} value is defined by the kinetic equation $dk^{ij}_{link} / d\varepsilon^{ij}_{eq} = -f(\varepsilon^{ij}_{eq}) < 0$. In the paper a function $f(\varepsilon^{ij}_{eq}) = 1/\varepsilon_{max}$ was used, where ε_{max} is input parameter of the model.

Simulation of formation or recovery chemical bond in unlinked (contact) pairs of movable cellular automata also is based on the use of criteria and the kinetic equation bond formation. In the paper the condition of achieving of the threshold (minimum) value of the compressive force in the pair was used as a criterion of bonding:

$$(-\sigma_{ij}) \ge \sigma^{min}_{link} \, , \tag{10}$$

where $\sigma_{link}^{\min}$ is input parameter of the model. If the condition (10) is satisfied, then the dynamics of the bonding is defined by the individual kinetic equation for k_{link}^{ij}. The work of plastic deformation ΔW_{ij} in the pair i and j at time step of numerical integration scheme is used as a parameter that determines the rate of the pair bonding:

$$\Delta k_{link}^{ij} = \frac{\Delta W_{ij}}{W_{\sigma}}, \tag{11}$$

where W_{σ} is the normalizing value, determined by the input parameters of the model and the current value of σ_{ij}:

$$W_{\sigma} = \frac{\left(-\sigma_{ij}\right) - \sigma_{link}^{\min}}{\sigma_{link}^{\max} - \sigma_{link}^{\min}} \left(W_{\sigma_{link}^{\min}} - W_{\sigma_{link}^{\min}}\right) + W_{\sigma_{link}^{\min}}. \tag{12}$$

Here $W_{\sigma_{link}^{\min}}$ is the total value of work of plastic deformation needed for complete bonding of the pair under the value of normal compression $\left(-\sigma_{ij}\right) = \sigma_{link}^{\min}$; $W_{\sigma_{link}^{\max}}$ is the total value of work of plastic deformation needed for complete bonding of the pair under the value of normal compression $\left(-\sigma_{ij}\right) = \sigma_{link}^{\max}$ (as a rule, $W_{\sigma_{link}^{\max}} < W_{\sigma_{link}^{\min}}$). Parameters $\sigma_{link}^{\min}$, $\sigma_{link}^{\max}$, $W_{\sigma_{link}^{\min}}$ and $W_{\sigma_{link}^{\max}}$ are the input parameters of the model ($\sigma_{link}^{\min} \le \sigma_{link}^{\max}$ and $W_{\sigma_{link}^{\max}} \le W_{\sigma_{link}^{\min}}$). Work of plastic deformation in pair *i-j* per one time step is defined as the sum of works in automata i and j: $\Delta W_{ij} = \Delta W_i + \Delta W_j$ [4-6].

Relations (1)-(12) make it possible to carry out an adequate numerical simulation of complex processes of elastoplastic deformation, fracture and bonding of fragments of metals during FSW process at the mesoscopic and macroscopic scales.

3 PROBLEM STATEMENT

To study the dynamics of the FSW process a 2D computer model in the framework of MCA method. The motion of a rigid non-destructive rotating disk (the working body or tool) along the interface of two metal plates (Me1 and Me2 in Fig. 1a) was considered. Plate dimensions were 10×25 mm (Fig. 1a). As working body was used disk of diameter 3 mm. In the initial position the tool was set at a distance of 8 mm from the left side of the modeled system (Fig. 1a). This choice of the initial position of the tool is determined by the need to minimize the influence of the lateral surfaces (in particular, the reflection of the elastic waves) on the dynamics of the FSW process. The elastic characteristics and the diagram of uniaxial loading of material were used as the input parameters of movable cellular automata. They determine the response function of the movable cellular automata. The response function of cellular automata simulating welded plates, characterized by elastic-plastic loading diagram with a linear hardening (Fig. 1d), was obtained by fitting of the diagram of uniaxial tension macroscopic samples of duralumin alloy.

Three-step loading scheme was used in the paper. In the first stage the initial stress state of the system was set through its hydrostatic compression with forces F_x and F_y (Fig. 1a). The necessity of this step is caused by the fact that in the work is modeled relatively small fragment of real system. In real FSW process movement of the tool lead to a spreading of a large amount of elastic waves in the plane of joined plates and, as a result, to appearing of significant elastic strains. Within the framework of the model these stresses were simulated by setting of the initial pressure, the value of which does not exceed the 20% of the yield stress of duralumin alloy.

In the second stage lateral, top and bottom surfaces of the modeled system were fixed (Fig. 1b) and the system was kept until the establishment of the force equilibrium.

In the third step simulation of the FSW process was carried out by movement of the tool with translational velocity V_{trans} along the line of the plates joint (Fig. 1c) and its rotation around the disc center with the angular velocity ω (an instantaneous linear speed to the disk surface was $V_{rot}=\omega R$, where R is the radius of the disk).

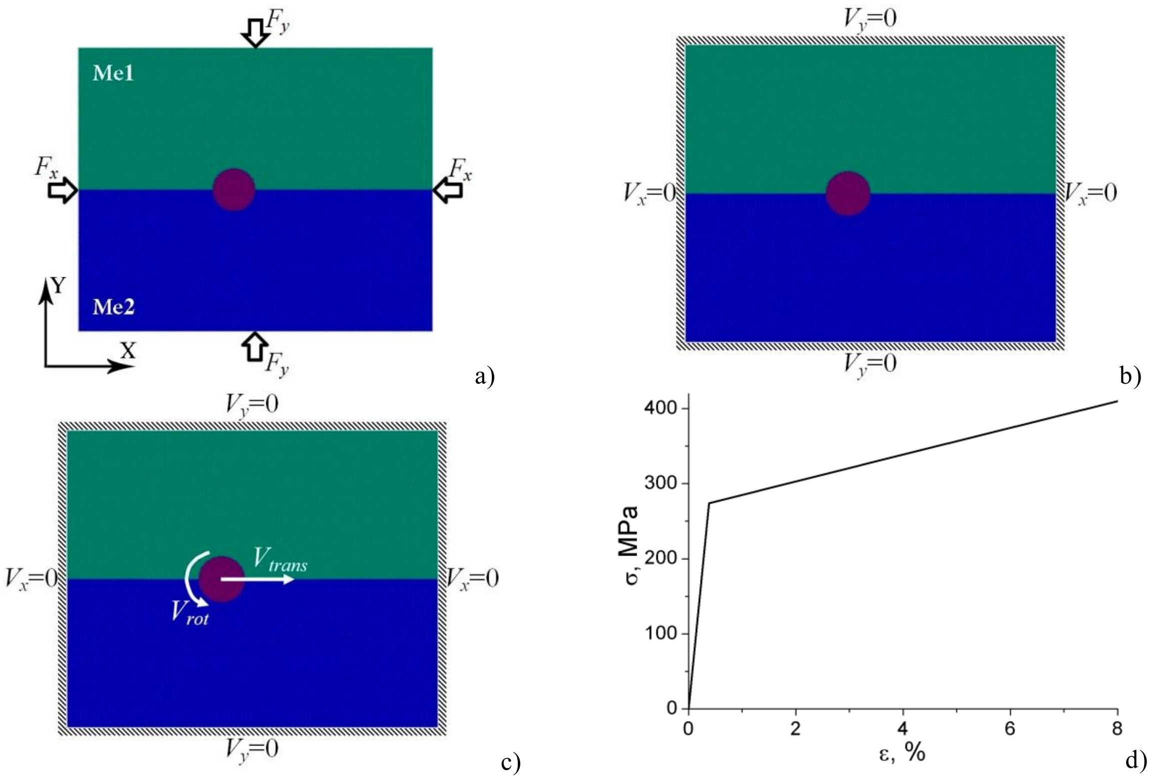

Figure 1: Loading scheme (a-c) and response function of duralumin plates (d).

4 RESULTS OF COMPUTER-AIDED SIMULATON

The dynamic of the FSW process was analyzed in the paper. In particular, the results of computer simulations show that at the beginning of the motion of the rotating tool occurs adhesion of duralumin alloy to the surface of working body, followed by separation of the substance in the vicinity of the contact welded plates and tool and active mixing of detached fragments (Fig. 2b). The subsequent movement of the tool is accompanied by further mixing of materials of the plates and transfer of the mixed substance from the frontal area (in Fig. 2 region on the right of the rotating tool) to the backcourt (Fig. 2c). This process is accompanied by formation of a welded joint (Fig. 2d). It is seen in Fig. 2 d that the trace from the passing of the tool consists of at least two parts. Directly behind the tool is observed an area in which take place processes of mixing of the substance and which are characterized by relatively high porosity. At a distance of about 1/6 of the tool radius, starting the area in which the mixing processes are completed. This zone is characterized by a relatively uniform distribution of the materials Me1 and Me2. It should be noted that the resulting welded joint is characterized by a small asymmetry relative to the line of the plates conjugation. Thus the width of the seam in the area below the conjugation line is approximately 7% higher than in the upper region (Fig. 2d). This result is in good agreement the experimental data [3].

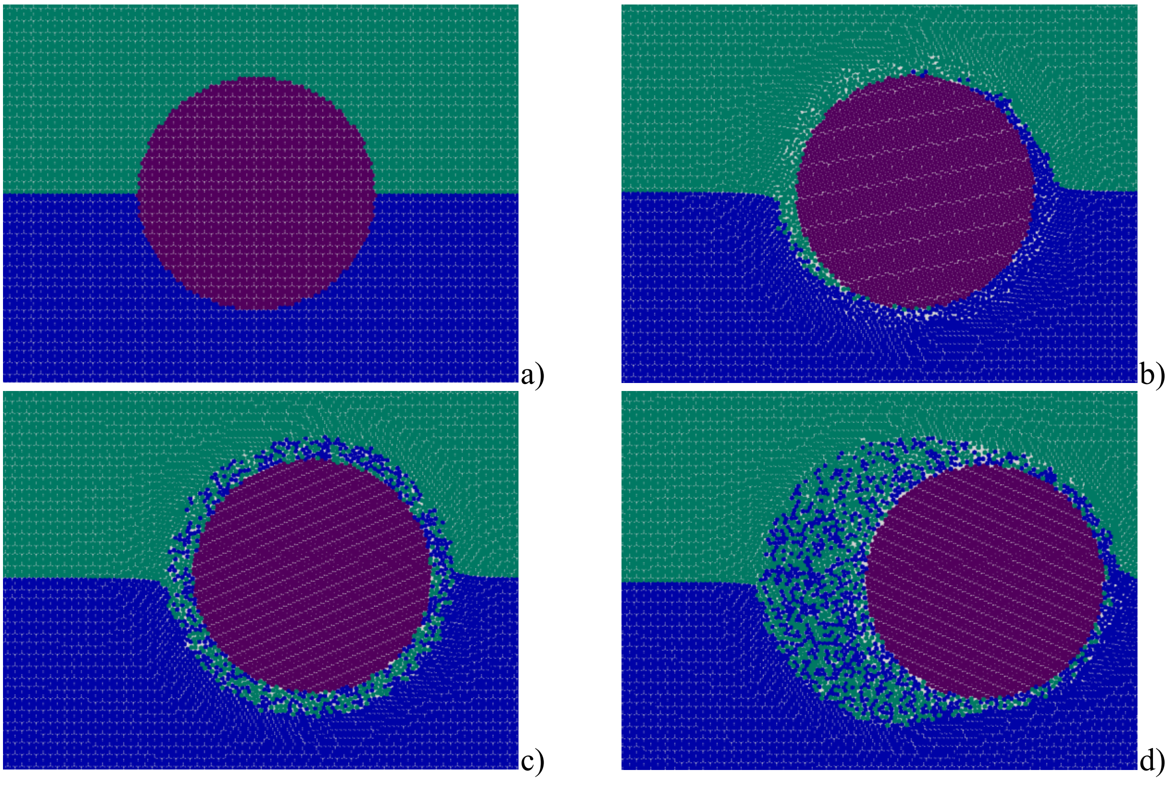

Figure 2: The structure of the material in the region of the rotating tool at various time points, V_{trans}=0,2 mps and V_{rot}=7,6 mps (ω=800 Hz): a) – t=0 s; b) – t=0,0004 s; c) – t=0,015 s; d) – t=0,07 s.

Analysis of the results of computer simulation showed that the quality of the welded joint is determined, in particular, by its friability (porosity), uniform volume distribution of welding materials, etc., is largely determined by the regime of movement of the tool (the ratio of the instantaneous speed of rotation of the tool surface V_{rot} to translational velocity V_{trans}). Figure 3 shows the structures of the resulting welded joints for three different regimes of the rotating tool movement. The figure shows that the decrease in V_{rot}/V_{trans} value (realized by increasing of the translational speed of the tool movement V_{trans}) leads to a decrease in the quality of welded joint. Thus, when V_{rot}/V_{trans}=38 (V_{rot}=7,6 mps, V_{trans}=0,2 mps, Fig. 3a), resulting welded joint is characterized by sufficiently low porosity (4.2 vol.%, Table 1), a small amount of planar defects (microcracks) and relatively uniform volume distribution of Me1 and Me2 materials in the upper and lower parts of the joint (Fig. 4a).

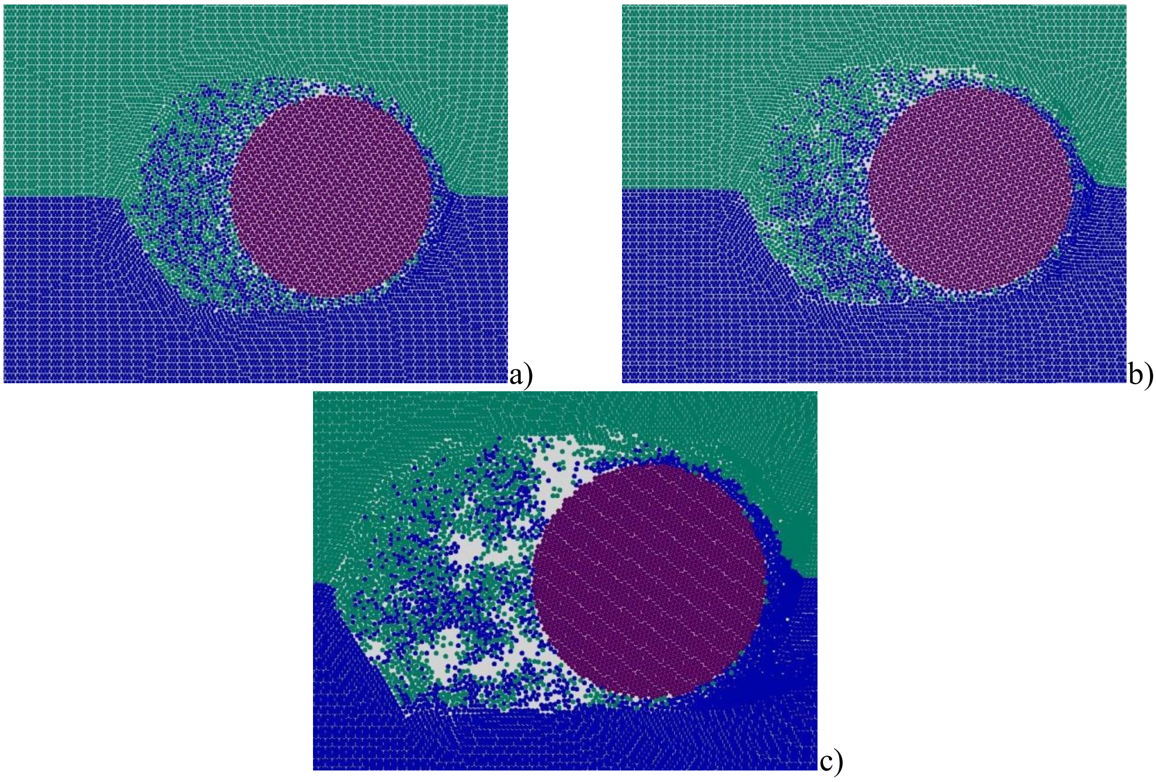

Figure 3: The structures of the resulting welded joint: a) - V_{rot}=7,6 mps (ω=800 Hz) and V_{trans}=0,2 mps; b) - V_{rot}=7,6 mps (ω=800 Hz) and V_{trans}=0,4 mps; c) - V_{rot}=7,6 mps (ω=800 Hz) and V_{trans}=0,8 mps.

Table 1: The porosity in the welded joint depending on the regime of the tool movement.

No. of regime	V_{rot}/V_{trans}	Porosity, vol.%
1	38 (V_{rot}=7,6 mps; V_{trans}=0,2 mps)	4,2
2	19 (V_{rot}=7,6 mps; V_{trans}=0,4 mps)	6,5
3	9,5 (V_{rot}=7,6 mps; V_{trans}=0,8 mps)	23,4

Twofold decrease of the V_{rot}/V_{trans} value (V_{rot}=7,6 mps, V_{trans}=0,4 mps, Fig. 3b) leads to increase in porosity of the joint (more than 1.5-fold, Table 1) and to a rather uneven distribution of Me1 and Me2 materials in the upper and lower parts of the joint (Fig. 4b). In this case the seam itself (especially the lower part) contains sufficiently large number of relatively extended microcracks. The consequence of further reducing of the ratio V_{rot}/V_{trans} ($Vrot$=7,6 mps, V_{trans}=0,8 mps, Fig. 3c) is the loss of continuity of the joint. It could be seen from Figure 3c that the seam can contain macropores and macro-cracks, even at a large distance from the rotating tool and the frontal area (in front of the working body) is characterizes by a significant seal (jam) of the material. The value of porosity in the backcourt reaches about 23.4.% (Table 1).

Thus, the synchronization of speeds of rotation and translational motion of rotating tool is one of the essential conditions for obtaining welded joint with a low content of pores and mikrocracks and uniform volumetric distribution of the welded materials.

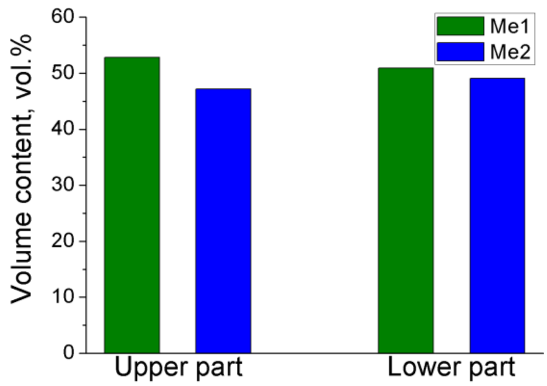

a)

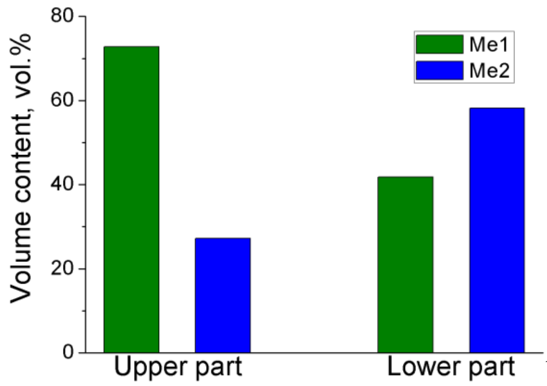

b)

Figure 4: The distribution of the volume fractions of materials Me1 and Me2 in the upper and lower parts of the welded joint: a) - V_{rot}=7,6 mps (ω=800 Hz) and V_{trans}=0,2 mps; b) - V_{rot}=7,6 mps (ω=800 Hz) and V_{trans}=0,4 mps.

5 CONCLUSIONS

Thus, in the paper adaptation of movable cellular automata method for studying the dynamics of the process of friction stir welding with a explicit account of the processes of fracture and formation of new chemical bonds was performed. Using the developed approach the dynamics of the process of friction stir welding of plates of duralumin alloy was investigated. It was shown that synchronization of speeds of rotation and translational motion of rotating tool is one of the essential conditions for obtaining welded joint with a low content of pores and mikrocracks and uniform volumetric distribution of the welded materials.

This work was supported by the Russian Science Foundation (Grant 14-19-00718). E.A. Kolubaev and S.G. Psakhie acknowledge financial support from the RF Ministry of Education and Science (project ID RFMEFI57814X0045) on “Improving the technology of friction stir welding by ultrasonic treatment to form permanent connections of hardened aluminum alloy for aerospace and transport industry”

REFERENCES

[1] Frolov, V.A., Ivanyukhin, A.N., Sabantsev, A.N. et. al Friction stir welding – pluses and minuses. *Welding International*. (2010) **24(5)**:358-365.

[2] Sergeeva, E.V. Friction stir welding in aerospace industry (rewiev). *The Paton Welding Journal*. (2013) **5**:56-60.

[3] Kolubaev, E.A. Investigation of the microstructure of joints of aluminum alloys produced by friction stir welding. *Russian Physics Journal*. (2015) **57(10)**:1321-1327.

[4] Psakhie, S., Shilko, E., Smolin, A. et al. Development of a formalism of movable cellular automaton method for numerical modeling of fracture of heterogeneous elastic-plastic materials. *Fract. Struct. Integrity* (2013) **24**:59-91.

[5] Psakhie, S.G., Shilko, E.V., Grigoriev, A.S. et al. A mathematical model of particle-particle interaction for discrete element based modeling of deformation and fracture of heterogeneous elastic-plastic materials. *Eng. Fract. Mech.* (2014) **130**:96-115.

[6] Shilko, E.V., Psakhie, S.G., Schmauder, S. et. al. Overcoming the limitations of distinct element method for multiscale modeling of materials with multimodal internal structure. Comp. Mat. Sci. (2015) 102:267-285.

[7] Psakhie, S., Ovcharenko, V., Baohai, Yu. et al. Influence of features of interphase boundaries on mechanical properties and fracture pattern in metal-ceramic composites. *J. Mater. Sci. Technol.* (2013) **29(11)**:1025-1034.

[8] Mustoe, G.G.W. A generalized formulation of the discrete element method. *Eng. Comp.* (1992) **9**:181-190.

[9] Bićanić, N. *Discrete element methods. In: E. Stein, R. Borst, T.J.R. Hughes (Eds.), Encyclopedia of computational mechanics*. Wiley, Chichester, Vol.1 (2004).

[10] Daw, M.S., Baskes, M.I. Embedded atom method: Derivation and application to impurities, surfaces, and other defects in metals. *Phys. Rev*. (1984) **B29(12)**:6443-6453.

[11] Rose, J.H., Smith, J.R., Guinea, F., Ferrante, J. Universal features of the equation of state of metals. *Phys. Rev*. (1984) **B29(6)**:2963-2969.

[12] Wilkins, M.L. *Computer simulation of dynamic phenomena*, Springer-Verlag, (1999).